# A State-Space Approach to Modelling DC Distribution Systems

van der Blij, Nils H.; Ramirez-Elizondo, Laura M.; Spaan, Matthijs T.J.; Bauer, Pavol

**DOI**
10.1109/TPWRS.2017.2691547

**Publication date**
2018

**Document Version**
Accepted author manuscript

**Published in**
IEEE Transactions on Power Systems

# A State-Space Approach to Modelling DC Distribution Systems

Nils H. van der Blij, *Student Member, IEEE,* Laura M. Ramirez-Elizondo, *Member, IEEE,* Matthijs T.J. Spaan, *Member, IEEE,* and Pavol Bauer, *Senior Member, IEEE*

***Abstract*—Many modelling methods for the analysis of dc distribution grids only consider monopolar configurations and do not allow for mutual couplings to be taken into account. The modelling method presented in this paper aims to deal with both of these issues. A state-space approach was chosen for its flexibility and computational speed. The derived approach can be applied to any dc distribution system regardless of its configuration and takes into account mutual couplings between phase conductors. Moreover, the state-space matrices can be derived in a programmatic manner. The derived model was verified empirically and by a reference model created in Simulink using PowerLib blocks. Subsequently, an illustrative system was analyzed, which showed the utility of the presented method in analyzing the dynamics of dc distribution systems. The presented method could especially be useful for the analysis, design and optimization of, for example, the stability and control systems of dc distribution systems.**

***Index Terms*—dc distribution, distribution line, dynamic analysis, microgrid, modelling, state-space.**

## I. Introduction

FUTURE distribution grids face major challenges such as growing energy demand and the introduction of intermittent distributed energy sources [1]. Microgrids could provide the flexibility needed for these integration of large amounts of distributed energy sources [2]. However, for ac microgrids it is often necessary to decouple their frequency from other networks (by, for example, a solid state transformer described in [3]), which increases complexity and cost. Therefore, the adequacy of ac and/or dc for future system architectures could be reevaluated. Furthermore, technological advances and societal concerns also indicate that a reevaluation of the current distribution system is timely [4]–[7]. Broad adoption of dc distribution systems still faces several challenges, mainly due to the strong market inertia of ac systems, lack of standardization for dc devices and systems, and insufficient experience with its protection and control [8].

Previous research into dc distribution systems presents several methods to analyze these systems. Examples of modelling monopolar dc distribution grids according to their transfer functions can be found in [9]–[11]. Furthermore, different state-space approaches to the modelling of dc distribution grids are discussed in [12]–[15]. Additionally, a transient (EMTP) approach to the distribution system can be found in [16]. However, these models only consider monopolar configurations and, when extended to other configurations, do not allow for mutual couplings to be taken into account.

In this paper a non-transient state-space approach is chosen because of its computational speed, flexibility, and ease of use. The creation of a transient simulation environment optimized for dc applications is still imperative for the transient analysis of dc distribution systems. The modelling method presented in [15] allows for the programmatic derivation of the state-space matrices from a so-called incidence matrix. However, this method was designed for monopolar (single phase conductor) grids, and the derivation does not allow for mutual couplings or conductance to ground to be taken into account. In this paper this model is modified and extended so that multiple phase conductors, mutual couplings and conductance to ground can be incorporated.

The contribution of this paper paper is a flexible generalized modelling method that simplifies the analysis, design, and optimization of dc distribution systems. The developed method is flexible enough to allow for the analysis of dc distribution systems with any number of nodes, distribution lines, and phase conductors, in any configuration. The novelty of the developed method lies in that it allows for multiple phase conductors, and that mutual couplings and conductance to ground can be taken into account. Furthermore, a procedure is presented how the matrices of a distribution system can be derived programmatically. Therefore, the method can be implemented in many simulation environments, and it allows for rapid analysis of different systems without the need of (re)building the model through a GUI.

The presented model is valid when the lines are much shorter than the wavelength(s) of the signals in the system. Therefore, the model can be used for any dc distribution (or transmission system) of any power rating as long as the above statement is true. Commercial simulation tools could produce similar results as the model. However, the mathematical nature of the presented model offers a significant advantage over these tools. It allows for the algebraic analysis of, for example, stability and control of dc distribution systems.

This paper is organized as follows: in Section II various modelling methods of (dc) distribution lines are reviewed. Section III presents the derivation of the developed state-space model. Section IV contains the validation of the developed model empirically and by using a simulation. Subsequently, Section V provides a dynamic analysis of an illustrative system. Lastly, in Section VI conclusions are drawn.

This project has received funding in the framework of the joint programming initiative ERA-Net Smart Grids Plus, with support from the European Union's Horizon 2020 research and innovation programme.

N. van der Blij, L. Ramirez-Elizondo, M. Spaan, and P. Bauer are with the Delft University of Technology, 2600 AA Delft, The Netherlands (e-mail: N.H.vanderblij@TUDelft.nl).

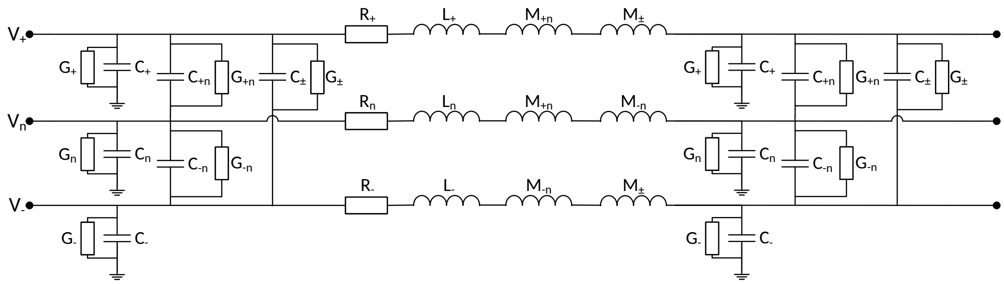


Fig. 1. Bipolar (three phase conductors) lumped element $\pi$ equivalent circuit of a distribution line including mutual couplings.

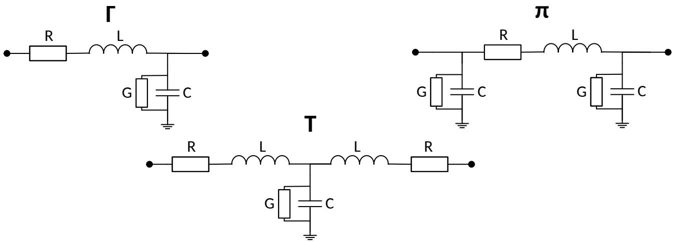


Fig. 2. $\Gamma$, $T$, and $\pi$ lumped element models of a distribution line.

## II. Distribution Line Models

Any dc distribution system consists of a number nodes which are interconnected by distribution lines. Often the power electronic converters, which are connected to the nodes, are modeled independently of the distribution lines. A plethora of modelling methods for distribution lines stem from the analysis of ac distribution systems. In general these methods can be subdivided into two categories; non-transient models and transient models.

### *A. Background: Non-Transient and Transient Models*

Non-transient models often assume a lumped element representation of the distribution line. Typically the $\Gamma$, $T$, or $\pi$ models, shown in Fig. 2, are used [17]. The lumped element models can be solved by, for example, their differential equations, transfer function, or a state-space representation. Several simulation environments exist where non-transient models of (dc) distribution lines are readily available such as MatLVDC, Simulink, Power Factory, and Modelica.

The limitations of (most) lumped element models lie in the neglect of propagation delays and frequency dependent effects. In general the parameters such as resistance, capacitance, conductance and inductance are assumed constant, while in reality they are frequency dependent. Moreover, it is usually assumed that changes at one side of the line are instantly discernible at the other side, while in reality there are propagation delays. The validity of neglecting propagation delays depends on the wavelength of the signal, which can be calculated by

$$\lambda = \frac{c}{f\sqrt{\epsilon_r \mu_r}}, \tag{1}$$

where $\lambda$ is the wavelength, $f$ is the frequency of the signal, $c$ is the speed of light, and $\epsilon_r$ and $\mu_r$ are the relative permittivity and relative permeability of the distribution line respectively. Usually it is assumed that propagation delays can be neglected when the length of the distribution line is much smaller than the wavelength of the signal [18].

Since transients such as short-circuits often impose high frequencies on the system, models that include propagation delays are often called transient models. The most common transient models are based on distributed lumped element models or travelling wave models. Some specialized transient simulation environments that implement these methods exist such as PSCAD-EMTDC, EMTP, and ATP. In general transient models are more accurate than non-transients models, but are much more complex and require much more computational power and time for a simulation.

To circumvent the problem of wavelengths becoming comparable to the lengths of the distribution lines the model can be broken up into smaller pieces which individually have lengths much shorter than the wavelength of the signal. However, solving such a segmented model could quickly become time consuming depending on the required number of subsections [19].

Other models directly take the propagation delay into account in their equations. Popular examples of such models are the Bergeron model and variants on the travelling wave model [19], [20]. For the latter it is required to fit the frequency response of the model to a set of rational functions.

### *B. DC Distribution Line Modelling*

Previous research on modelling dc distribution grids focuses mostly on monopolar (single phase conductor) dc distribution system architectures. However, since dc ground currents cause corrosion it is unlikely to only have a single distribution line in practice [21]. Moreover, bipolar grids are becoming more common, further increasing the likelihood of multiple phase conductors. The presence of multiple phase conductors introduces mutual couplings in the form of mutual inductance, conductance, and capacitance between the phase conductors. These couplings can have a significant effect on the dynamics of the system depending on the characteristics of the distribution lines. Furthermore, the conductance with respect to ground is usually not taken into account. While for overhead lines this can mostly be neglected, for underground cables the effect of conductance can be significant.

In this paper the distribution lines are modeled in a lumped element $\pi$ configuration that includes mutual couplings. An example of this model for a bipolar (three phase conductors) distribution line is shown in Fig. 1.

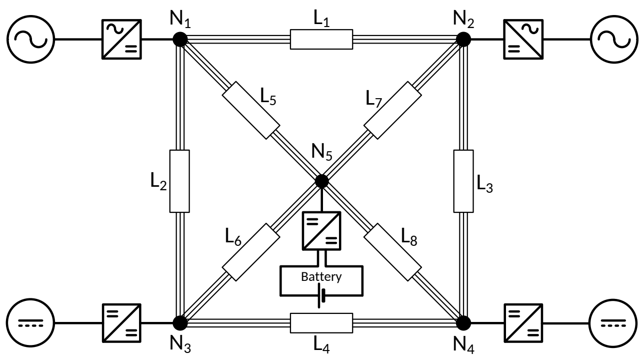


Fig. 3. Example of a bipolar dc distribution system containing storage, and dc and ac loads/sources.

## III. Universal State-Space Approach

An example of a dc distribution system is shown in Fig. 3. In general any dc distribution system can be described by its $n$ nodes, $l$ distribution lines and $m$ phase conductors. In this section a state-space model is derived that can be utilized for any dc distribution system.

### A. Distribution Network Model

To model the distribution system using a state-space approach the state variables must be chosen. These variables must fully describe the system, but fewer variables result in lower computation times. For this model the state variables are chosen to be the voltages at each node and the currents in each distribution line. The formulae for these voltages and currents are

$$\boldsymbol{C}\dot{\boldsymbol{U}}_{\boldsymbol{N}} = \sum \boldsymbol{I}_{\boldsymbol{N}}, \tag{2}$$

$$\boldsymbol{L}\dot{\boldsymbol{I}}_{\boldsymbol{L}} = \boldsymbol{\Delta U}_{\boldsymbol{L}}, \tag{3}$$

where $\boldsymbol{U_N}$ are the voltages at each node, $\boldsymbol{I_N}$ are the net currents flowing into each node, $\boldsymbol{I_L}$ are the currents flowing in each distribution line, $\boldsymbol{\Delta U_L}$ are the voltage drops over each distribution line's inductance, and $\boldsymbol{C}$ and $\boldsymbol{L}$ are the matrices for the capacitance and inductance of the network respectively. Here, and for the remainder of this paper, dot notation indicates a time derivative of that variable and bold face of variables indicates that they are vectors or matrices.

The net current flowing into each node consists of the current from the connected load or source, the current from connected distribution lines, and current leaked through admittances. Similarly the voltage drop over the inductance of the distribution line relates to the voltage difference between the two connected nodes and the voltage drop over the distribution line's resistance. Therefore, by substituting these quantities into (2) and (3) we arrive at

$$\boldsymbol{C}\dot{\boldsymbol{U}}_{\boldsymbol{N}} = \boldsymbol{I}_{\boldsymbol{DC}} - \boldsymbol{I}'^{\,T}_{\boldsymbol{m}}\boldsymbol{I}_{\boldsymbol{L}} - \boldsymbol{G}\boldsymbol{U}_{\boldsymbol{N}}, \tag{4}$$

$$\boldsymbol{L}\dot{\boldsymbol{I}}_{\boldsymbol{L}} = \boldsymbol{I}'_{\boldsymbol{m}}\boldsymbol{U}_{\boldsymbol{N}} - \boldsymbol{R}\boldsymbol{I}_{\boldsymbol{L}}, \tag{5}$$

where $\boldsymbol{I_{DC}}$ are the currents flowing from the connected sources and loads, $\boldsymbol{I'_m}$ is the multi phase conductor incidence matrix, and $\boldsymbol{G}$ and $\boldsymbol{R}$ are the matrices for the conductance and resistance of the network respectively.

The incidence matrix depicts the interconnections between the nodes in the network while the multi phase conductor incidence matrix extends this matrix by creating a node for each phase conductor at each node of the incidence matrix. The incidence matrix and the multi phase conductor incidence matrix are given by

$$\boldsymbol{I_m}(j,i) = \begin{cases} 1 & \text{if } I_j \text{ is flowing from node } i \\ -1 & \text{if } I_j \text{ is flowing in node } i \end{cases}, \tag{6}$$

$$\boldsymbol{I'_m}((j-1)m+k,(i-1)m+k) = \boldsymbol{I_m}(j,i), \tag{7}$$

where the total number of nodes, distribution lines and phase conductors are depicted by $n$, $l$, and $m$ respectively. Moreover, one must cycle through all index combinations of nodes ($i$), distribution lines ($j$), and phase conductors ($k$) to create the complete incidence matrices.

With the inverses of the capacitance and inductance matrices the state-space equations can be derived to be

$$\dot{\boldsymbol{U}}_{\boldsymbol{N}} = \boldsymbol{C}^{-1}\boldsymbol{I}_{\boldsymbol{DC}} - \boldsymbol{C}^{-1}\boldsymbol{I}'^{\,T}_{\boldsymbol{m}}\boldsymbol{I}_{\boldsymbol{L}} - \boldsymbol{C}^{-1}\boldsymbol{G}\boldsymbol{U}_{\boldsymbol{N}}, \tag{8}$$

$$\dot{\boldsymbol{I}}_{\boldsymbol{L}} = \boldsymbol{L}^{-1}\boldsymbol{I}'_{\boldsymbol{m}}\boldsymbol{U}_{\boldsymbol{N}} - \boldsymbol{L}^{-1}\boldsymbol{R}\boldsymbol{I}_{\boldsymbol{L}}. \tag{9}$$

To solve these state-space equations they need to be molded into the form of

$$\dot{\boldsymbol{x}} = \boldsymbol{A}\boldsymbol{x} + \boldsymbol{B}\boldsymbol{u}, \tag{10}$$

$$\boldsymbol{y} = \boldsymbol{C}\boldsymbol{x} + \boldsymbol{D}\boldsymbol{u}, \tag{11}$$

where $\boldsymbol{x}$ is the set of state variables, $\boldsymbol{u}$ is the set of input variables, $\boldsymbol{y}$ are the output variables, and $\boldsymbol{A}$, $\boldsymbol{B}$, $\boldsymbol{C}$ and $\boldsymbol{D}$ are the state-space matrices. The state variables and input variables for different phase conductors are grouped by node or line, and are composed as

$$\boldsymbol{x} = \begin{bmatrix} U_{1,1} & U_{1,2} & \cdots & U_{n,m} & I_{1,1} & \cdots & I_{n,m} \end{bmatrix}, \tag{12}$$

$$\boldsymbol{u} = \begin{bmatrix} I_{DC,1,1} & I_{DC,1,2} & \cdots & I_{DC,l,m} \end{bmatrix}, \tag{13}$$

where $U_{i,k}$ is the voltage of the phase conductor $k$ at node $i$, and $I_{DC,j,k}$ is the current flowing in phase conductor $k$ of distribution line $j$.

The $\boldsymbol{A}$, $\boldsymbol{B}$, $\boldsymbol{C}$, and $\boldsymbol{D}$ matrices can now be derived from (8) and (9) and are given by

$$\boldsymbol{A} = \begin{bmatrix} \boldsymbol{A_{11}} & \boldsymbol{A_{12}} \\ \boldsymbol{A_{21}} & \boldsymbol{A_{22}} \end{bmatrix}, \tag{14}$$

$$\boldsymbol{A_{11}} = -\boldsymbol{C}^{-1}\boldsymbol{G}, \tag{15}$$

$$\boldsymbol{A_{12}} = -\boldsymbol{C}^{-1}\boldsymbol{I}'^{\,T}_{\boldsymbol{m}}, \tag{16}$$

$$\boldsymbol{A_{21}} = \boldsymbol{L}^{-1}\boldsymbol{I}'_{\boldsymbol{m}}, \tag{17}$$

$$\boldsymbol{A_{22}} = -\boldsymbol{L}^{-1}\boldsymbol{R}, \tag{18}$$

$$\boldsymbol{B} = \begin{bmatrix} \boldsymbol{B_{11}} \\ \boldsymbol{B_{21}} \end{bmatrix}, \tag{19}$$

$$\boldsymbol{B_{11}} = \boldsymbol{C}^{-1}, \tag{20}$$

$$\boldsymbol{B_{21}} = \emptyset, \tag{21}$$

$$\boldsymbol{C} = \boldsymbol{I}, \tag{22}$$

$$\boldsymbol{D} = \emptyset, \tag{23}$$

where $\emptyset$ indicates an empty matrix and $\boldsymbol{I}$ indicates an identity matrix.

The impedance and admittance matrices $\boldsymbol{C}$, $\boldsymbol{L}$, $\boldsymbol{G}$ and $\boldsymbol{R}$ can be formed by employing (24) to (33). Firstly, the impedance and admittance matrices of all distribution lines, including (mutual) couplings between different phase conductors, are depicted as

$$\boldsymbol{R_{L,j}} = \begin{bmatrix} R_1 & 0 & \cdots & 0 \\ 0 & \ddots & \ddots & \vdots \\ \vdots & \ddots & \ddots & 0 \\ 0 & \cdots & 0 & R_m \end{bmatrix}, \tag{24}$$

$$\boldsymbol{L_{L,j}} = \begin{bmatrix} L_{11} & M_{12} & \cdots & M_{1m} \\ M_{21} & \ddots & \ddots & \vdots \\ \vdots & \ddots & \ddots & M_{(m-1)m} \\ M_{m1} & \cdots & M_{m(m-1)} & L_{mm} \end{bmatrix}, \tag{25}$$

$$\boldsymbol{C_{L,j}} = \begin{bmatrix} \sum_{k=1}^{m} C_{1k} & -C_{12} & \cdots & -C_{1m} \\ -C_{21} & \ddots & \ddots & \vdots \\ \vdots & \ddots & \ddots & -C_{(m-1)m} \\ -C_{m1} & \cdots & -C_{m(m-1)} & \sum_{k=1}^{m} C_{mk} \end{bmatrix}, \tag{26}$$

$$\boldsymbol{G_{L,j}} = \begin{bmatrix} \sum_{k=1}^{m} G_{1k} & -G_{12} & \cdots & -G_{1m} \\ -G_{21} & \ddots & \ddots & \vdots \\ \vdots & \ddots & \ddots & -G_{(m-1)m} \\ -G_{m1} & \cdots & -G_{m(m-1)} & \sum_{k=1}^{m} G_{mk} \end{bmatrix}, \tag{27}$$

where the components of $\boldsymbol{R_{L,j}}$ $\boldsymbol{L_{L,j}}$, $\boldsymbol{C_{L,j}}$ and $\boldsymbol{G_{L,j}}$ indicate the resistance, (mutual) inductance, capacitance and conductance between the phase conductors of each distribution line.

Since a form of $\pi$-model is used the capacitance and conductance matrices of each node can be found by summing half of the capacitance and conductance of each distribution line connected to it:

$$\boldsymbol{C_{N,i}} = \frac{1}{2}\sum_{j=1}^{l} \boldsymbol{C_{L,j}} \; [I_m(j,i) \neq 0], \tag{28}$$

$$\boldsymbol{G_{N,i}} = \frac{1}{2}\sum_{j=1}^{l} \boldsymbol{G_{L,j}} \; [I_m(j,i) \neq 0]. \tag{29}$$

If any external capacitance or conductance (such as grounding) is added to the network these could also be incorporated in these equations.

Finally, the impedance and admittance matrices that are used in the state-space equations can be formed:

$$\boldsymbol{R} = \begin{bmatrix} \boldsymbol{R_{L,1}} & 0 & \cdots & 0 \\ 0 & \ddots & \ddots & \vdots \\ \vdots & \ddots & \ddots & 0 \\ 0 & \cdots & 0 & \boldsymbol{R_{L,l}} \end{bmatrix}, \tag{30}$$

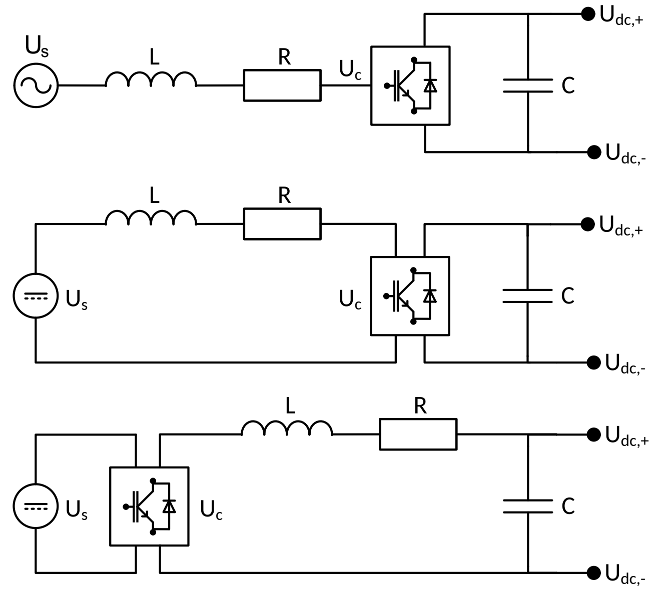


Fig. 4. Simplified diagrams of ac/dc, boost, and buck converters.

$$\boldsymbol{L} = \begin{bmatrix} \boldsymbol{L_{L,1}} & 0 & \cdots & 0 \\ 0 & \ddots & \ddots & \vdots \\ \vdots & \ddots & \ddots & 0 \\ 0 & \cdots & 0 & \boldsymbol{L_{L,l}} \end{bmatrix}, \tag{31}$$

$$\boldsymbol{C} = \begin{bmatrix} \boldsymbol{C_{N,1}} & 0 & \cdots & 0 \\ 0 & \ddots & \ddots & \vdots \\ \vdots & \ddots & \ddots & 0 \\ 0 & \cdots & 0 & \boldsymbol{C_{N,n}} \end{bmatrix}, \tag{32}$$

$$\boldsymbol{G} = \begin{bmatrix} \boldsymbol{G_{N,1}} & 0 & \cdots & 0 \\ 0 & \ddots & \ddots & \vdots \\ \vdots & \ddots & \ddots & 0 \\ 0 & \cdots & 0 & \boldsymbol{G_{N,n}} \end{bmatrix}. \tag{33}$$

### B. Converter Model

The presented state-space method for the distribution network allows for the employment of any convenient converter model. Nonetheless, this subsection presents a simple (universal) state-space model for ac/dc, boost, and buck converters which can be implemented together with the distribution network model.

Simplified diagrams of ac/dc, boost and buck converters are shown in Fig. 4. For the ac/dc converter the q-axis of the dq-frame is assumed to be aligned with the ac voltage through a PLL. Consequently, for all converters the (d-axis) voltage across the inductor and resistor determines the current flowing in the inductor. Therefore, the current flowing in the inductor and voltage across the capacitor are calculated according to

$$\dot{i}_L = \frac{\Delta U}{L} - \frac{R}{L} i, \tag{34}$$

$$\dot{U}_{dc} = \frac{K}{C} i, \tag{35}$$

where $i_L$ is the current flowing in the inductor, $\Delta U$ is the voltage across the inductor and resistor, $U_{dc}$ is the voltage of the (secondary side) capacitor, and the factor $K$ conserves the power across the primary and secondary side of the converter (for example, $K = U_c/U_{dc}$ for the ac/dc converter). Unfortunately, for a state-space approach the factor $K$ needs to be linearized.

An inner control loop for the current, and an outer control loop for the voltage or power is employed. The equations for both (PI) controllers, in case the voltage is controlled, are

$$\Delta U = \left(\frac{K_{i,1}}{s} + K_{p,1}\right)(i_L^* - i_L), \tag{36}$$

$$i_L^* = \left(\frac{K_{i,2}}{s} + K_{p,2}\right)(U_{dc}^* - U_{dc}), \tag{37}$$

where $K_{i,1}$ and $K_{i,2}$ are the integral gains of the controllers, $K_{p,1}$ and $K_{p,2}$ are the proportional gains of the controllers, and $i_L^*$ and $U_{dc}^*$ are the reference values of the inductor current and capacitor voltage respectively.

To implement these controllers a state variable is required for the current controller ($\alpha$) and for the voltage controller ($\beta$). The chosen equations for these state variables are

$$\dot{\alpha} = K_{i,1}(i_L^* - i_L), \tag{38}$$

$$\dot{\beta} = K_{i,2}(U_{dc}^* - U_{dc}). \tag{39}$$

By substituting (38) and (39) into (36) and (37) we arrive at the following equations:

$$\Delta U = \alpha - K_{p,1} i_L + K_{p,1}K_{p,2}(U_{dc}^* - U_{dc}) + K_{p,1}\beta, \tag{40}$$

$$i_L^* = \beta - K_{p,2}U_{dc} + K_{p,2}U_{dc}^*. \tag{41}$$

Finally, the state-space equations can be derived by substituting (40) and (41) into (34) and (35). The state-space equations for the converter are then given by

$$\begin{bmatrix} \dot{i}_L \\ \dot{U}_{dc} \\ \dot{\alpha} \\ \dot{\beta} \end{bmatrix} = \boldsymbol{A} \begin{bmatrix} i_L \\ U_{dc} \\ \alpha \\ \beta \end{bmatrix} + \boldsymbol{B} U_{dc}^*, \tag{42}$$

$$\begin{bmatrix} i_L \\ U_{dc} \end{bmatrix} = \boldsymbol{C} \begin{bmatrix} i_L \\ U_{dc} \\ \alpha \\ \beta \end{bmatrix} + \boldsymbol{D} U_{dc}^*, \tag{43}$$

$$\boldsymbol{A} = \begin{bmatrix} \frac{-R}{L} - \frac{K_{p,1}}{L} & \frac{-K_{p,1}K_{p,2}}{L} & \frac{1}{L} & \frac{K_{p,1}}{L} \\ \frac{K}{C} & 0 & 0 & 0 \\ -K_{i,1} & -K_{i,1}K_{p,2} & 0 & K_{i,1} \\ 0 & -K_{i,2} & 0 & 0 \end{bmatrix}, \tag{44}$$

$$\boldsymbol{B} = \begin{bmatrix} \frac{K_{p,1}K_{p,2}}{L} \\ 0 \\ K_{i,1}K_{p,2} \\ K_{i,2} \end{bmatrix}, \tag{45}$$

$$\boldsymbol{C} = \begin{bmatrix} 1 & 0 & 0 & 0 \\ 0 & 1 & 0 & 0 \end{bmatrix}, \tag{46}$$

$$\boldsymbol{D} = \emptyset. \tag{47}$$

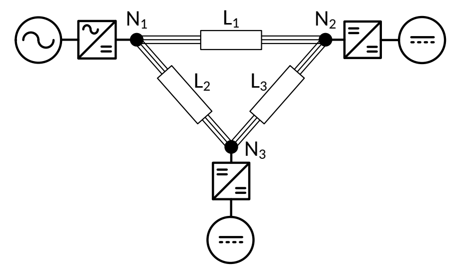


Fig. 5. Reference bipolar network used for the verification of the state-space model.

## IV. Model Validation

The validity of the derived state-model is verified using a reference system shown in Fig. 5. In this network the ac/dc converter controls the voltage of the bipolar distribution network. The dc/dc converters represent a load and a source in the network. For the distribution lines three 1 km cables were used of which the mutual couplings were significantly increased to better verify the model for their effect on the system dynamics.

For the verification, an equivalent electrical network was built using PowerLib blocks in Simulink. To ensure an optimal comparison, both the developed state-space model and the PowerLib model were implemented in parallel in the same Simulink model. Consequently, identical time-steps are taken for both models. Moreover, to prevent the feedback loops of the converters from enhancing any discrepancies between the models, the converters and their control were modeled separately from the network and their output was provided to both models.

The verification scenario that is used can be found in Table I. In addition to a step in the voltage and power control signals, a short-circuit is induced at the node of the ac/dc controller at $t = 15$ ms. In Fig. 6 the output of the state-space model as a result of the verification scenario is shown.

TABLE I
VERIFICATION SCENARIO FOR THE STATE-SPACE MODEL

| $t$ [ms] | $U_{dc}^*$ [V] | $P_1^*$ [W] | $P_2^*$ [W] | Short-circuit |
|---|---|---|---|---|
| 0 | 700 | 0 | 0 | No |
| 5 | 800 | 0 | 0 | No |
| 10 | 800 | 3200 | -3200 | No |
| 15 | 800 | 3200 | -3200 | Yes |
| 20 | 800 | 3200 | -3200 | Yes |

From Fig. 6 several empirical verifications can be done. For example, it can be seen that the voltages of the nodes of the same pole conductor start to differ slightly as a result of a step in power. Furthermore, during the short-circuit the voltages of the neutral conductor drop quickly due to the capacitance between the poles and the neutral. Afterwards, the neutral voltages return to 0 V because of the conductance between the neutral and ground. Interestingly, the neutral current does not react much to a fast change in the pole currents (as a result of mutual inductance) due to the effect of the capacitance at both sides of the distribution line.

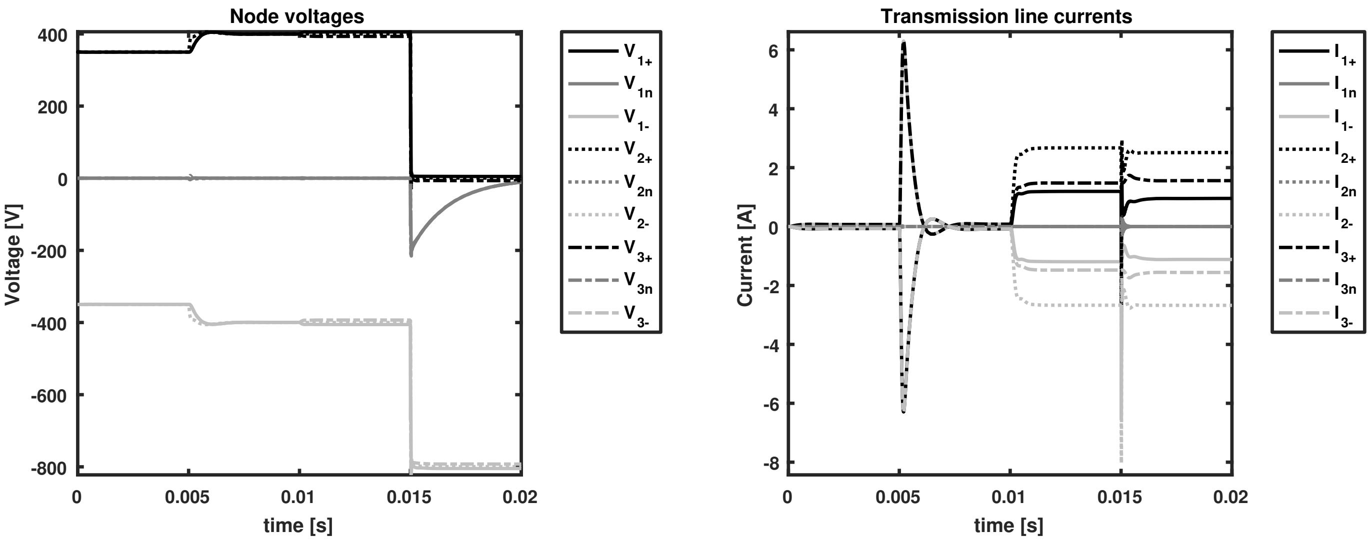


Fig. 6. Node voltages and distribution line currents of the state-space model as a result of the verification scenario.

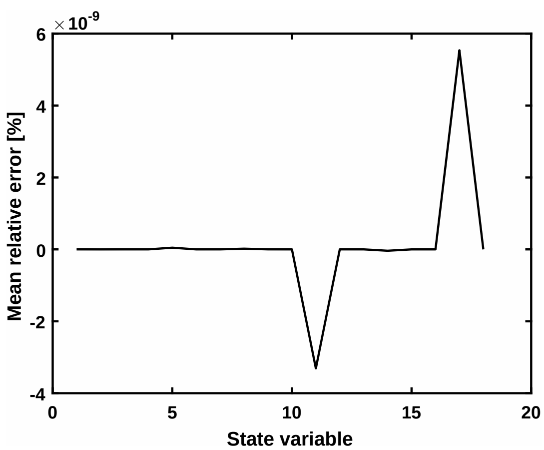


Fig. 7. Mean relative error of the state-space model compared to the PowerLib model as a result of the verification scenario.

A more quantified verification can be done when comparing the results of the state-space model and the PowerLib model. The error between the two models did not go above $10^{-11}$ (Volt or Ampere) for any of the state variables during any moment of the verification scenario. As a summary the mean relative error for all 18 state variables is given in Fig. 7. From this graph it can be seen that the error between the two models is negligible. Please note that the spikes in the mean relative error are caused by variables that remain close to zero throughout the simulation.

This model has comparable accuracy for other dc distribution systems (regardless of power or configuration) as long as long as the lines are much shorter than the wavelength(s) of the signals and the frequency dependent components of the impedance and admittance can be neglected.

## V. Simulation of a Bipolar Distribution Grid

In the previous section the validity of the state-space model was verified. In this section a more complex example of a bipolar dc distribution system is modelled and investigated.

The schematic of an illustrative distribution system is shown in Fig. 9. At the node in the middle ($N_1$) the voltage of the distribution system is controlled, while the converters at the other nodes control their own output/input power. The incidence matrix for this network can be derived from the figure and is given by

$$I_m = \begin{bmatrix} 1 & -1 & 0 & 0 & 0 \\ 1 & 0 & -1 & 0 & 0 \\ 1 & 0 & 0 & -1 & 0 \\ 1 & 0 & 0 & 0 & -1 \\ 0 & 1 & -1 & 0 & 0 \\ 0 & -1 & 0 & 1 & 0 \\ 0 & 0 & 1 & 0 & -1 \\ 0 & 0 & 0 & -1 & 1 \end{bmatrix}. \tag{48}$$

The scenario for which this distribution grid will be investigated is shown in Table II. First, the voltage will be stepped up, after which the various nodes will change their output/input power at varying times.

TABLE II
SCENARIO FOR THE ILLUSTRATIVE DISTRIBUTION SYSTEM

| $t$ [ms] | $U_{dc}^*$ [V] | $P_2^*$ [W] | $P_3^*$ [W] | $P_4^*$ [W] | $P_5^*$ [W] |
|---|---|---|---|---|---|
| 0 | 700 | 0 | 0 | 0 | 0 |
| 5 | 750 | 0 | 0 | 0 | 0 |
| 10 | 750 | 1500 | 0 | 0 | -1500 |
| 15 | 750 | 1500 | -3000 | 0 | -1500 |
| 20 | 750 | 1500 | -3000 | 2250 | -1500 |
| 25 | 750 | 1500 | -3000 | 2250 | -1500 |

The resulting voltages of the nodes and the currents in the distribution lines for the positive pole conductor are shown in Fig. 8. In the previous section it was shown that as long as no short-circuit occurs (and the system is balanced) little happens in the neutral voltages and currents. Furthermore, the negative pole quantities would, in this case, be identical but opposite in sign to the positive pole quantities.

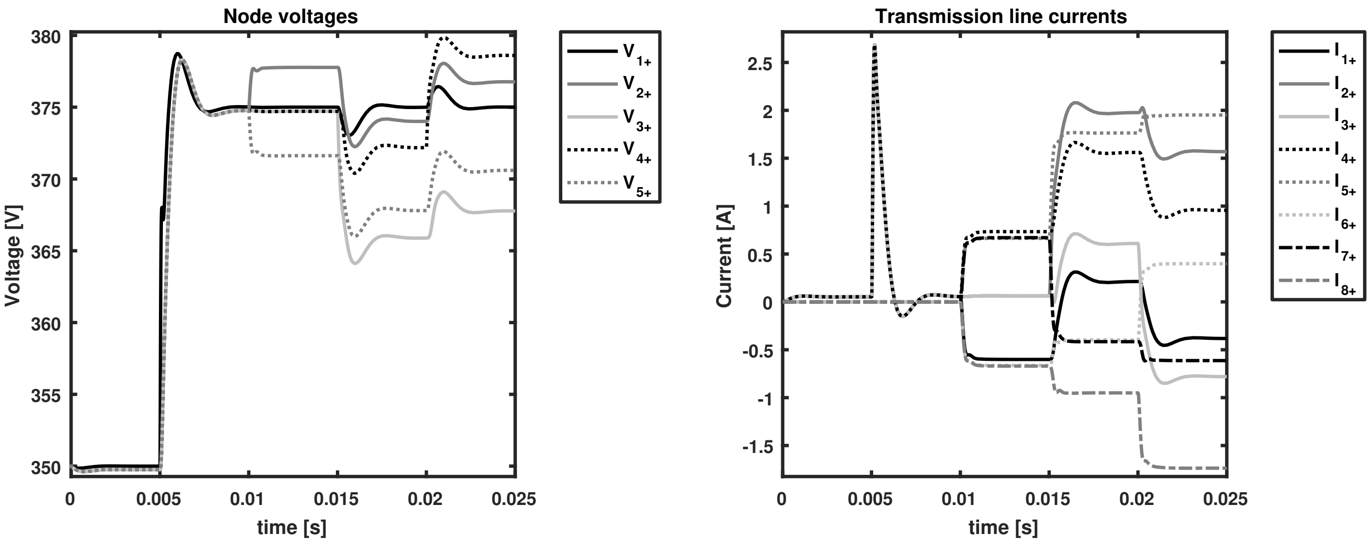


Fig. 8. Node voltages and distribution line currents of the illustrative bipolar dc distribution grid for the given scenario.

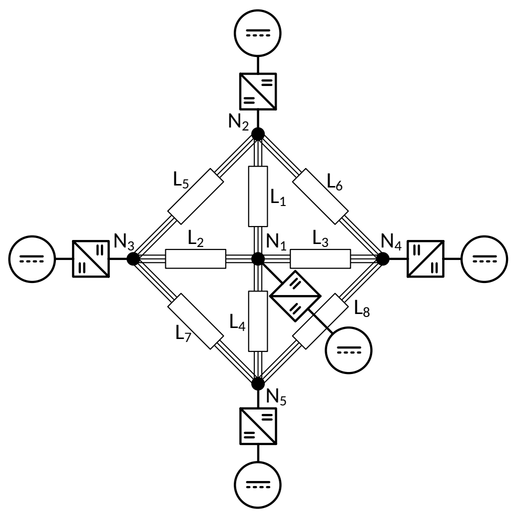


Fig. 9. Illustrative bipolar dc distribution grid for the demonstration of the state-space model.

From the voltage and current overshoot it can be seen that the inner and outer controllers of the converter are tightly tuned. Additionally, at the start of the simulation a slight transient can be observed that is caused by the conductance to ground of the distribution lines.

Since the network is connected in star with respect to the voltage regulator and is otherwise symmetrical, during the step up in voltage, the currents $I_{1+}$ to $I_{4+}$ are equal while the currents $I_{5+}$ to $I_{8+}$ are zero. Subsequently, during the symmetrical load step in $N_2$ and $N_5$ the voltages $V_{1+}$ and $V_{5+}$ get offset respectively, while the currents get distributed over all distribution lines other than $L_2$ and $L_3$. When at 15 ms a load is introduced in the system which is not directly compensated by an equal source, the average voltage in the distribution system drops, while the currents flowing from $N_1$ increase significantly. Finally, when the load is partly compensated by another source the average voltage rises again.

From this example it is clear the developed modelling technique is useful for the dynamic analysis of dc distribution systems. The validity of the presented model only depends on the wavelength(s) (see Section II) of the signals and therefore does not depend on the power rating of the system. The model is flexible enough to extend with more complex and more compelling scenarios, converter models, and control schemes (for example, droop control). Furthermore, the presented modeling method could be used to algebraically analyze the stability and control of dc distribution systems.

## VI. Conclusion

This paper discussed the need for a novel and flexible modelling method for the dynamic analysis of dc distribution systems. Starting from previous research in modelling dc distribution systems and the comparison of different modelling methods used for ac lines, a choice for a non-transient state-space approach was made. The derived state-space approach can be applied to dc distribution systems with any number of phase conductors, nodes, and distribution lines, in any configuration. Furthermore, this model can be applied regardless of power rating and is also valid for transmission systems as long as the wavelength(s) of the signals are significantly smaller than the line lengths. Moreover, the state-space matrices of this model can be created programmatically, resulting in an easy to use method.

The model was verified using built in electrical components from PowerLib in Simulink. The PowerLib model showed strong congruency with the derived state-space model proving its validity. Moreover, the derived model behaved as expected during voltage, power, and short-circuit dynamics. Subsequently, a more complex distribution system was analyzed to showcase what the model can be used for.

In conclusion, this paper presents a flexible, accurate, and fast modeling method to analyze the dynamics of dc distribution systems. The state-space approach could in the future be used for the mathematical analysis, design, and optimization of, for example, control systems in dc distribution systems.

## REFERENCES

[1] A. Ipakchi and F. Albuyeh, "Grid of the future," *IEEE Power and Energy Magazine*, vol. 7, no. 2, pp. 52–62, March 2009.

[2] X. Liu and B. Su, "Microgrids x2014; an integration of renewable energy technologies," in *2008 China International Conference on Electricity Distribution*, Dec 2008, pp. 1–7.

[3] Y. Du, S. Baek, S. Bhattacharya, and A. Q. Huang, "High-voltage high-frequency transformer design for a 7.2kv to 120v/240v 20kva solid state transformer," in *IECON 2010 - 36th Annual Conference on IEEE Industrial Electronics Society*, Nov 2010, pp. 493–498.

[4] "Smart grid: reinventing the electric power system," IEEE Power and Energy Magazine for Electric Power Professionals, IEEE Power and Energy Society, 2012.

[5] J. W. Coltman, "The transformer [historical overview]," *IEEE Industry Applications Magazine*, vol. 8, no. 1, pp. 8–15, Jan 2002.

[6] T. McNichol, *AC/DC: The savage tale of the first standards war*. John Wiley & Sons, 2011.

[7] D. M. Larruskain, I. Zamora, O. Abarrategui, and Z. Aginako, "Conversion of {AC} distribution lines into {DC} lines to upgrade transmission capacity," *Electric Power Systems Research*, vol. 81, no. 7, pp. 1341 – 1348, 2011.

[8] L. Mackay, T. G. Hailu, G. C. Mouli, L. Ramrez-Elizondo, J. A. Ferreira, and P. Bauer, "From dc nano- and microgrids towards the universal dc distribution system - a plea to think further into the future," in *2015 IEEE Power Energy Society General Meeting*, July 2015, pp. 1–5.

[9] A. P. N. Tahim, D. J. Pagano, E. Lenz, and V. Stramosk, "Modeling and stability analysis of islanded dc microgrids under droop control," *IEEE Transactions on Power Electronics*, vol. 30, no. 8, pp. 4597–4607, Aug 2015.

[10] T. Hailu, L. Mackay, L. Ramirez-Elizondo, J. Gu, and J. A. Ferreira, "Voltage weak dc microgrid," in *DC Microgrids (ICDCM), 2015 IEEE First International Conference on*, June 2015, pp. 138–143.

[11] Q. Shafiee, T. Dragicevic, J. C. Vasquez, and J. M. Guerrero, "Modeling, stability analysis and active stabilization of multiple dc-microgrid clusters," in *Energy Conference (ENERGYCON), 2014 IEEE International*, May 2014, pp. 1284–1290.

[12] S. Anand and B. G. Fernandes, "Reduced-order model and stability analysis of low-voltage dc microgrid," *IEEE Transactions on Industrial Electronics*, vol. 60, no. 11, pp. 5040–5049, Nov 2013.

[13] M. T. Dat, G. V. den Broeck, and J. Driesen, "Modeling the dynamics of a dc distribution grid integrated of renewable energy sources," in *IECON 2014 - 40th Annual Conference of the IEEE Industrial Electronics Society*, Oct 2014, pp. 5559–5564.

[14] M. K. Zadeh, R. Gavagsaz-Ghoachani, J. P. Martin, S. Pierfederici, B. Nahid-Mobarakeh, and M. Molinas, "Discrete-time modelling, stability analysis, and active stabilization of dc distribution systems with constant power loads," in *2015 IEEE Applied Power Electronics Conference and Exposition (APEC)*, March 2015, pp. 323–329.

[15] P. B. Silvio Rodrigues, Rodrigo Teixeira Pinto, *Dynamic Modeling and Control of VSC-based Multi-terminal DC Networks*, 1st ed. Lambert Academic Publishing, 2012.

[16] J. Han, Y.-S. Oh, G.-H. Gwon, D.-U. Kim, C.-H. Noh, T.-H. Jung, S.-J. Lee, and C.-H. Kim, "Modeling and analysis of a low-voltage dc distribution system," *Resources*, vol. 4, no. 3, p. 713, 2015. [Online]. Available: http://www.mdpi.com/2079-9276/4/3/713

[17] T. Dhaene and D. de Zutter, "Selection of lumped element models for coupled lossy transmission lines," *IEEE Transactions on Computer-Aided Design of Integrated Circuits and Systems*, vol. 11, no. 7, pp. 805–815, Jul 1992.

[18] C. R. Paul, *Analysis of Multiconductor Transmission Lines*, 2nd ed. Wiley-IEEE Press, 2007.

[19] R. M. D. B. B. Gustavsen, G. Irwin and K. Kent, "Transmission line models for the simulation of interaction phenomena between parallel ac and dc overhead lines," *International Conference on Power System Transients*, vol. 11, no. 7, pp. 805–815, Jul 1992.

[20] J. Yang, J. O'Reilly, and J. E. Fletcher, "An overview of dc cable modelling for fault analysis of vsc-hvdc transmission systems," in *Universities Power Engineering Conference (AUPEC), 2010 20th Australasian*, Dec 2010, pp. 1–5.

[21] J. J. Justo, F. Mwasilu, J. Lee, and J.-W. Jung, "Ac-microgrids versus dc-microgrids with distributed energy resources: A review," *Renewable and Sustainable Energy Reviews*, vol. 24, pp. 387 – 405, 2013.

**Nils H. van der Blij** was born in Leiden in the Netherlands, on March 11, 1990. He received his electrical engineering bachelor and master degree from the Delft University of Technology in 2011 and 2013 respectively. His research experience includes Scarabee, Philips, Cambridge University, and Delft University of Technology. His specializations lie in the field of dc distribution grids, electrical machines and drives, and sustainable energy generation. He is currently a PhD candidate working on the management and control of dc distribution grids.

**Dr. Laura Ramirez-Elizondo** is assistant professor at the DC Systems, Energy Conversion & Storage group. In 2003, she received her bachelors degree in Electrical Engineering and her bachelors degree in Music with a major in Piano at the Universidad de Costa Rica. She graduated with honors from her M.Sc. studies in Electrical Power Engineering at Delft University of Technology in 2007. She holds a PhD in eletrical engineering from the Delft University of Technology (2013).

**Dr. Matthijs Spaan** is an assistant professor of Computer Science at Delft University of Technology, the Netherlands. He holds a PhD degree in Computer Science (2006) and an MSc degree in Artificial Intelligence (2002), both from the University of Amsterdam.

**Prof. Dr. Pavol Bauer** is currently a full Professor with the Department of Electrical Sustainable Energy 0f Delft University of Technology and head of DC Systems, Energy Conversion and Storage group. He published over 72 journal and almost 300 conference papers in his field (with H factor Google scholar 30, Web of science 18), he is an author or co-author of 8 books, holds 4 international patents and organized several tutorials at the international conferences. He has worked on many projects for industry concerning wind and wave energy, power electronic applications for power systems such as Smarttrafo; HVDC and LV DC systems, projects for smart cities such as PV charging of electric vehicles, PV and storage integration, contactless charging; and he participated in several Leonardo da Vinci and H2020 EU projects as project partner (ELINA, INETELE, E-Pragmatic) and coordinator (PEMCWebLab.com-Edipe, SustEner, Eranet DCMicro). He is a Senior Member of the IEEE, former chairman of Benelux IEEE Joint Industry Applications Society, Power Electronics and Power Engineering Society chapter, chairman of the Power Electronics and Motion Control (PEMC) council, member of the Executive Committee of European Power Electronics Association (EPE) and also member of international steering committee at numerous conferences.